Tunable ferroelectric domain wall alignment in strained monoclinic $K_XNa_{1-X}NbO_3$ epitaxial films

D. Braun, M. Schmidbauer, M. Hanke, A. Kwasniewski, and J. Schwarzkopf

Citation: Appl. Phys. Lett. **110**, 232903 (2017); doi: 10.1063/1.4985191
View online: http://dx.doi.org/10.1063/1.4985191
View Table of Contents: http://aip.scitation.org/toc/apl/110/23
Published by the American Institute of Physics

Tunable ferroelectric domain wall alignment in strained monoclinic $K_xNa_{1-x}NbO_3$ epitaxial films

D. Braun,[1,a)] M. Schmidbauer,[1] M. Hanke,[2] A. Kwasniewski,[1] and J. Schwarzkopf[1]
[1]*Leibniz Institute for Crystal Growth, D-12489 Berlin, Germany*
[2]*Paul-Drude Institute for Solid State Electronics, D-10117 Berlin, Germany*

(Received 3 April 2017; accepted 26 May 2017; published online 9 June 2017)

Epitaxial growth of ferroelectric $K_xNa_{1-x}NbO_3$ thin films on (110) $NdScO_3$ substrates results in the formation of domain walls which significantly differ in their arrangement from commonly observed 45° or 90° inclinations. The deviation is attributed to the monoclinic symmetry of the evolving a_1a_2/M_C herringbone pattern and can be controlled by the epitaxial strain. In this work, tuning of the in-plane domain angle is systematically performed by the variation of the potassium content in $K_xNa_{1-x}NbO_3$. The experimental data are in full agreement with a theoretical model. The observed behavior yields a promising pathway for domain engineering and patterning of periodic structures. *Published by AIP Publishing.* [http://dx.doi.org/10.1063/1.4985191]

In nanoscale technological applications using ferroelectrics, the availability of materials with enhanced piezoelectric properties is highly requested. In particular, such an enhancement can be achieved by using materials in which the electrical polarization vector can continuously rotate within symmetry planes of the respective crystal unit cell. Such a freedom is exclusively attributed to low symmetry monoclinic phases in which the monoclinic mirror plane is the primary symmetry element. Indeed, this phenomenon was initially observed at the morphotropic phase boundary (MPB) of lead zirconium titanate where the unit cell symmetry changes from rhombohedral to tetragonal[1–3] via a monoclinic bridging phase enabling giant piezoelectric responses. However, beyond this aspect of enhanced piezoelectric properties, which is essentially well understood, it would be also highly desirable to provide a material system which exhibits a tunable domain wall arrangement. This ability has been rarely investigated yet, but would lead to an increased versatility of applicable ferroelectric domain pattern.

In common ferroelectric materials with tetragonal or orthorhombic symmetry, the electrical polarization vector is linked to a crystallographic axis. As a result of this restriction, the corresponding domain walls can be tilted against the main crystallographic axes exclusively by angles of 45° or 90°,[4,5] although the angle between both adjacent polarization vectors could be different as apparent in rhombohedral systems.[6,7] The permitted domain wall angles are strongly coupled to the symmetry of the crystal unit cell and are controlled by the compatibility of adjacent unit cells at the domain walls. Remarkably, for ferroelectric systems with monoclinic symmetry, the domain walls can be arranged in arbitrary directions and the included angle can be almost continuously modified. In a theoretical work, Bokov and Ye[8] showed that the domain wall angles may vary in the range of several tens of degree. They basically depend only on the lattice parameters and the monoclinic angle. Therefore, the realization of monoclinic phases would provide the combination of a highly piezo active and simultaneously flexible domain pattern.

The use of a ferroelectric material with monoclinic symmetry thus enables a promising route for "domain engineering" through implementation of an additional degree of freedom. Indeed, such a flexible domain pattern would give rise to a wide range of technological applications.

For instance, tailored periodic templates are requested to pattern the device on top.[9] In this way, exemplary nanostructures for an increased storage density[10] can be arranged in a more flexible way. This has been, e.g., demonstrated for metallic nanowires on $LiNbO_3$.[11] Moreover, a nanoscale ferroelectric herringbone pattern is discussed for the use in energy harvesting devices[12] and for applications requiring a tunable thermal conductivity.[13] In all these applications, a flexible domain wall arrangement would be beneficial. However, such a behavior has not been experimentally confirmed for monoclinic systems yet.

In the present work, we will demonstrate that targeted adjustment of the monoclinic unit cell can be used to systematically vary the corresponding domain wall angles. For that purpose, we have chosen the $K_xNa_{1-x}NbO_3$ material system which has been shown to be a promising candidate to create ferroelectric monoclinic domains of large versatility. For example, a highly periodic monoclinic stripe domain pattern can be obtained for $NaNbO_3$[14] and $K_{0.75}Na_{0.25}NbO_3$[15] epitaxial thin films grown on (110) $TbScO_3$ orthorhombic substrates. Moreover, the potassium atomic concentration x can be adjusted in such a way that two monoclinic phases differing in surface orientation can be simultaneously achieved. This coexistence was demonstrated for $K_{0.9}Na_{0.1}NbO_3$ grown on (110) $NdScO_3$ and is a result of an elastic strain energy density degeneration.[16] As a consequence of this multi-domain state, a characteristic herringbone pattern evolves whose inclination angle will be investigated in the present study. Through a variation of the potassium content x between $x = 0.80$ to 0.95 in $K_xNa_{1-x}NbO_3$ thin films on $NdScO_3$ substrates the spatial dimension as well as the shearing angle of the monoclinic unit cell can be modified. The comparatively narrow composition range is based on the

a)dorothee.braun@ikz-berlin.de

requirement of coexisting a_1a_2 and M_c phases with *Pm* symmetry which induces a pronounced herringbone domain pattern.[16] However, despite the small variation in the potassium content x the monoclinic distortion angle β and the vertical lattice parameter do change significantly. We will show that this will lead to distinct modifications of the domain wall angle, which is in excellent agreement with the theoretical model introduced by Bokov and Ye.[8]

All samples shown were grown by liquid-delivery spin metal-organic chemical vapor phase deposition (MOCVD). The huge advantage of this technique is the epitaxial growth close to thermodynamic equilibrium accompanied by a comparatively high oxygen partial pressure. As a result, fully strained and stoichiometric films with smooth surfaces and interfaces are obtained. For more details, see Refs. 15 and 17. In order to avoid premature plastic strain relaxation, the films were deposited directly on the (110) $NdScO_3$ substrates without a bottom electrode in-between. The film thickness was limited to 20–30 nm which is well below the critical thickness of plastic relaxation thus guaranteeing fully strained films.

The surface morphology of the films was analyzed via atomic force microscopy (AFM; Asylum Research MFP-3D stand-alone instrument). The surface topology (not shown here) of all films exhibits rather smooth surfaces with a root mean square roughness well below 0.5 nm. The ferroelectric domain structure was investigated within the piezoresponse force microscopy (PFM) mode embedded as dual AC resonance tracking (DART) version. Lateral piezoresponse images of all samples are shown in Figs. 1(a)–1(d).

In accordance with linear elasticity theory,[16] coexistence of a_1a_2 and M_C domains is observed which is interlaced to a herringbone pattern. The well-defined stripe domains with domain walls tilted by an angle α against the $[001]_{NSO}$ direction are additionally enclosed in bundles along $[001]_{NSO}$ [see inset in Fig. 1(b)]. Since the arrangement is identical for the lateral and the vertical PFM image, the dark and bright domains can be identified as alternating monoclinic a_1a_2/M_c domain structure in reference to Schmidbauer *et al.*[16] Obviously, the stripe domains do not include an angle of 45° or 90° to the $[001]_{NSO}$ directions (as it would be expected for orthorhombic or tetragonal films[4,5,18]). In order to quantitatively evaluate the inclination angles, α_{PFM}^{exp}, of the stripe domains, we have performed a two-dimensional Fourier analysis of the PFM images shown in Figs. 1(a)–1(d). We found that they systematically vary between 49° (x = 0.80) and 76° (x = 0.90) with the film composition x. In order to correlate this result with the monoclinicity of the film unit cell, the monoclinic shearing angle β was determined. For this purpose, grazing incidence in-plane x-ray diffraction (GIXD) has been performed at station BM20 of the European Synchrotron (ESRF, Grenoble, France) and at KMC-2 beamline of Bessy II (Helmholtz Center, Berlin, Germany). For these measurements, the glancing angle of incidence was chosen slightly above the critical angle of total external reflection. This leads to a strong suppression of the substrate Bragg reflection and to maximum sensitivity for the thin film signal. Two-dimensional in-plane reciprocal space maps were recorded by using a one-dimensional position sensitive detector aligned parallel to the sample surface.

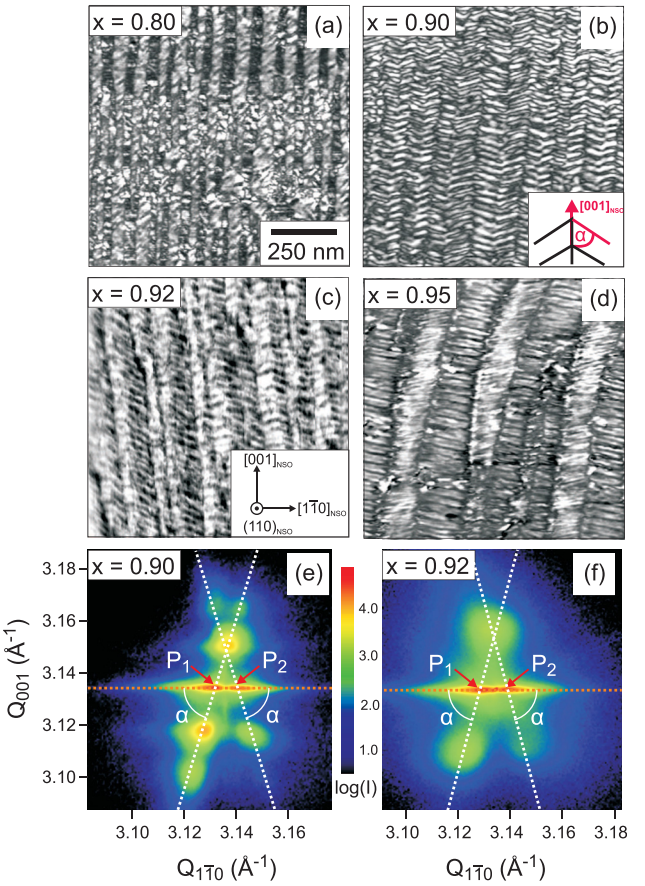

FIG. 1. (a)–(d) Lateral piezoresponse force amplitude images ($1 \times 1\ \mu m$) of $K_xNa_{1-x}NbO_3$ films grown on (110) $NdScO_3$ orthorhombic substrate with varying potassium concentration x. Insets in (b) and (c) show the definition of in-plane domain wall inclination angle α and the orientation of the $NdScO_3$ substrate, respectively. (e) and (f) Grazing incidence in-plane x-ray diffraction intensity distribution recorded in the vicinity of the $(2\bar{2}4)_{NSO}$ reciprocal lattice point for x = 0.90 and x = 0.92, respectively.

This advanced multi-detection technique enables fast two-dimensional reciprocal space mappings with excellent counting statistics.[19] In order to distinguish between strain and morphology related features in reciprocal space, a variety of Bragg reflections – e.g., $(004)_{NSO}$, $(008)_{NSO}$, and $(2\bar{2}4)_{NSO}$ – was investigated.

As an example, two selected in-plane intensity distributions recorded in the vicinity of the $(2\bar{2}4)_{NSO}$ reciprocal lattice point are presented in Figs. 1(e) and 1(f) for two samples with potassium contents of x = 0.90 and x = 0.92, respectively. A complicated diffraction pattern evolves for both samples. The periodic arrangement of the domain walls leads to two inclined intensity branches (marked by white dashed lines) which are intersected by broad correlation peaks. From the inclination of the two branches, the domain wall angle α_{GIXD}^{exp} is obtained [indicated in Figs. 1(e) and 1(f)]. Moreover, the separation $\Delta Q_{1\bar{1}0}$ of the central peaks P_1 and P_2 of the two branches is related to the monoclinic distortion angle β via

$$\tan\beta = \frac{\Delta Q_{1\bar{1}0}}{2Q_{001}}. \quad (1)$$

The corresponding β angles are summarized in Table I.

The experimental domain wall angles obtained from PFM (α_{PFM}^{exp}) and GIXD (α_{GIXD}^{exp}) analysis are illustrated in

TABLE I. Structural parameters of the samples under investigation. The in-plane lattice parameters of the film are equal to the in-plane lattice parameters of the (110) $NdScO_3$ surface unit cell ($d_{1\bar{1}0} = 4.0124$ Å and $d_{001} = 4.0025$ Å).

	Sample 1	Sample 2	Sample 3	Sample 4
K atomic concentration x	0.80	0.90	0.92	0.95
Vertical lattice spacing d (Å)	3.969	3.986	3.989	3.992
Monoclinic angle β (deg)	0.145	0.11	0.08	0.077

Fig. 2 as blue circles and red triangles, respectively, as a function of monoclinic distortion β.

The error bars result from the reading accuracy. It is striking that (i) the experimental data evaluated from PFM and GIXD are in excellent agreement and (ii) the domain wall angle is quite sensitive to the monoclinic distortion of the film unit cell.

The correlation between monoclinic shearing angle β and in-plane domain wall angle α has been theoretically considered by Fousek *et al.*[20] for the arrangement of compatible ferroelectric domain walls depending on their respective symmetry and by Sapriel[21] for ferroelastics. The special case of monoclinic symmetry was discussed later by Bokov and Ye.[8] On the basis of these geometrical considerations, compatible monoclinic domain walls can be identified and the resulting domain wall angles α can be derived for *Pm* symmetry. Thereby, two different domain walls S_1 and S_2 can appear whose plane equations are denoted as follows:

$$\begin{array}{cc} S_1\ walls & S_2\ walls \\ (a-b)(x \pm y) = \pm 2dz & (c-a)(x \pm y) = \pm 2dz. \end{array} \quad (2)$$

The difference is a quantitative change of the tilting angle of the domain wall around the pseudocubic (pc) $\langle 001 \rangle_{pc}$ directions. In Eq. (2), the parameter set *a*, *b*, *c*, and *d* denotes the components of the so-called spontaneous strain tensor.[22] These quantities can be expressed by the pseudocubic[23] lattice parameters a_{pc}, b_{pc}, and c_{pc} and the monoclinic distortion angle β via

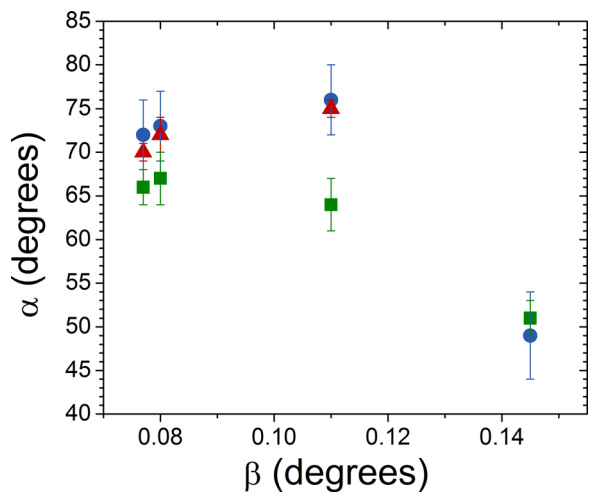

FIG. 2. In-plane domain wall inclination angle α derived from PFM (blue circle) and GIXD (red triangle) along with calculated values (green square) as a function of the monoclinic distortion angle β (for details see text).

$$a = \frac{b_{pc} - p}{p}, \quad b = \frac{a_{pc} - p}{p}, \quad c = \frac{c_{pc} - p}{p},$$
$$2d = \frac{\pi}{2} - \beta, \quad p = \frac{a_{pc} + b_{pc} + c_{pc}}{3}. \quad (3)$$

Furthermore, x, y, and z describe likewise the main crystallographic axes as well as the indices of the planes in the pseudocubic notation. The domain wall angle α with respect to the $\langle 001 \rangle_{pc}$ directions can be evaluated as traces of these walls on, e.g., the x = 0 planes via

$$\begin{array}{cc} S_1\ walls & S_2\ walls \\ \tan\alpha_1 = \dfrac{a-b}{\pm 2d} & \tan\alpha_2 = \dfrac{c-a}{\pm 2d}. \end{array} \quad (4)$$

The monoclinic shearing angle β (exaggerated plotted) and the domain wall inclination angle α are sketched in Fig. 3.

For fully strained films, the dimensions of the surface unit cell of the $NdScO_3$ substrate can be used as in-plane lattice parameters of the film, while the vertical lattice parameters have been determined from $\theta/2\theta$ high resolution x-ray diffraction scans (see Table I). Introducing these values in Eqs. (3) and (4), the domain wall angles α^{theo} were calculated and are displayed in Fig. 2 as green squares with error bars given by the experimental uncertainties of β. Very good qualitative and quantitative agreement between experimental and calculated values is achieved. However, minor differences can still be observed. In general, the theoretical descriptions[8,20] assume a single-domain and free-standing crystal. In consequence, no epitaxial stresses are considered as they apply for the fully strained films discussed in this work. Mokrý and Fousek[24] have calculated the impact of

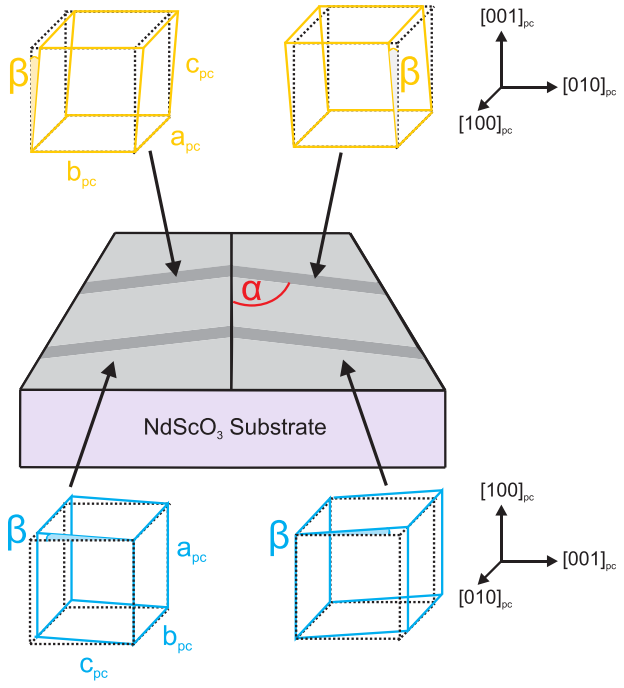

FIG. 3. Schematic view of the domain pattern with embedded domain wall inclination angle α and the respective $K_xNa_{1-x}NbO_3$ (sheared) pseudocubic unit cells (cross sectional view). The monoclinic a_1a_2 domains with $(100)_{pc}$ orientation are colored in blue, the M_C domains with $(001)_{pc}$ orientation are depicted with yellow color. The monoclinic distortion angle β is illustrated for both orientations and shearing directions.

elastic stresses resulting from domain wall alignment in the case of more than two ferroelectric/ferroelastic domains. They found that in the presence of the so-called "domain quadruplets" the ferroelastic domains prohibit a stress-free coexistence. Indeed, the a_1a_2 and M_c domains exhibit different monoclinic distortions requiring an elastic relaxation process at the domain walls. As a result, the pure geometric aspects of the models given in Refs. 8 and 20 do not correctly reflect the true experimental conditions and a deviation from the prediction seems reasonable.

Nevertheless, the results demonstrate that the domain wall angles in a herringbone pattern can be tuned by varying the lattice parameter of the epitaxially grown $K_xNa_{1-x}NbO_3$ thin films. In this context, it also has to be considered that the monoclinic distortion β varies with film thickness.[14,25] Above the critical thickness of plastic relaxation, the lattice parameters of a fully strained film relax to those of an unstrained film crucially influencing the domain pattern. The thickness dependence of the herringbone domain pattern goes beyond the scope of this letter and will be presented in a future paper.

In summary, we have shown that the domain wall angle in a herringbone pattern in monoclinic $K_xNa_{1-x}NbO_3$ thin films can significantly deviate from 45° or 90°. For epitaxially strained $K_xNa_{1-x}NbO_3$ films on (110) $NdScO_3$ substrates, it could even be verified that the domain wall alignment is flexible and can be adjusted according to the theoretical model of Bokov and Ye.[8] Within a potassium concentration range between $x = 0.80$ and 0.95, domain wall angles between 49° and 76° could be experimentally obtained. Thereby, a decisive difference is derived for the $K_xNa_{1-x}NbO_3$ system in comparison to tetragonal, orthorhombic, or rhombohedral systems, where domain walls are exclusively arranged along main crystallographic axes. This emphasizes the outstanding role of monoclinic phases in ferroelectric materials. This symmetry inherent property to tilt the domain walls nearly arbitrarily against main crystallographic axes results in an additional degree of freedom with regard to "domain engineering" and allows for targeted manipulation of the ferroelectric, periodic domain pattern on a nanometer scale.

We thank ESRF for providing beam time in the framework of project MA-2604 and Helmholtz Center Berlin for project 15202778. We are grateful to Valentina Cantelli and Daniel Többens for assistance with the x-ray diffraction experiments and to M. Klann for MOCVD sample growth. The $NdScO_3$ substrates have been grown in Leibniz Institute for Crystal Growth (group of R. Uecker) and have been prepared for growth by company CrysTec.

[1]H. Fu and R. E. Cohen, Nature **403**, 281 (2000).
[2]R. Guo, L. E. Cross, S.-E. Park, B. Noheda, D. E. Cox, and G. Shirane, Phys. Rev. Lett. **84**, 5423 (2000).
[3]B. Noheda and D. E. Cox, Phase Transitions **79**, 5 (2006).
[4]A. S. Everhardt, S. Matzen, N. Domingo, G. Catalan, and B. Noheda, Adv. Electron. Mater. **2**, 1500214 (2016).
[5]B. Meyer and D. Vanderbilt, Phys. Rev. B **65**, 104111 (2002).
[6]A. Lubk, S. Gemming, and N. A. Spaldin, Phys. Rev. B **80**, 104110 (2009).
[7]P. Marton, I. Rychetsky, and J. Hlinka, Phys. Rev. B **81**, 144125 (2010).
[8]A. A. Bokov and Z.-G. Ye, J. Appl. Phys. **95**, 6347 (2004).
[9]P. R. Potnis, N. T. Tsou, and J. E. Huber, Materials **4**, 417 (2011).
[10]G. Catalan, A. Schilling, J. F. Scott, and J. M. Gregg, J. Phys.: Condens. Matter **19**, 132201 (2007).
[11]J. N. Hanson, B. J. Rodriguez, R. J. Nemanich, and A. Gruverman, Nanotechnology **17**, 4946 (2006).
[12]A. R. Balakrishna and J. E. Huber, Smart Mater. Struct. **25**, 104001 (2016).
[13]J. J. Wang, Y. Wang, J. F. Ihlefeld, P. E. Hopkins, and L. Q. Chen, Acta Mater. **111**, 220 (2016).
[14]A. Duk, M. Schmidbauer, and J. Schwarzkopf, Appl. Phys. Lett. **102**, 091903 (2013).
[15]J. Schwarzkopf, D. Braun, M. Hanke, A. Kwasniewski, J. Sellmann, and M. Schmidbauer, J. Appl. Cryst. **49**, 375 (2016).
[16]M. Schmidbauer, D. Braun, T. Markurt, M. Hanke, and J. Schwarzkopf, Nanotechnology **28**, 24LT02 (2017).
[17]J. Schwarzkopf, M. Schmidbauer, T. Remmele, A. Duk, A. Kwasniewski, S. B. Anooz, A. Devi, and R. Fornari, J. Appl. Cryst. **45**, 1015 (2012).
[18]R. R. P. Kumari, S. Sharma, M. Shandilya, and A. Tiwari, Adv. Mater. Lett. **6**, 453 (2015).
[19]M. Schmidbauer, P. Schäfer, S. Besedin, D. Grigoriev, R. Köhler, and M. Hanke, J. Synchrotron Radiat. **15**, 549 (2008).
[20]J. Fousek and V. Janovec, J. Appl. Phys. **40**, 135 (1969).
[21]J. Sapriel, Phys. Rev. B **12**, 5128 (1975).
[22]K. Aizu, J. Phys. Soc. Jpn. **28**, 706 (1970).
[23]A. Vailionis, H. Boschker, W. Siemons, E. P. Houwman, D. A. Blank, G. Rijnders, and G. Koster, Phys. Rev. B **83**, 064101 (2011).
[24]P. Mokrý and J. Fousek, J. Appl. Phys. **97**, 114104 (2005).
[25]M. Schmidbauer, J. Sellmann, D. Braun, A. Kwasniewski, A. Duk, and J. Schwarzkopf, Phys. Status Solidi RRL **8**, 522 (2014).